Kinetic Part-Feeding Models for Assembly Lines in Automotive Industries

Michael Herty, Lena Michailidis and Marcus Ziegler

Preprint No. 397 **June 2014**

Key words: network dynamics, kinetic theory, asymptotic analysis

AMS Subject Classifications: 58F15, 58F17, 53C35

Institut für Geometrie und Praktische Mathematik
RWTH Aachen

Templergraben 55, D-52056 Aachen, (Germany)

RWTH Aachen University, Templergraben 55, 52056 Aachen, Germany, herty@igpm.rwth-aachen.de.
Daimler AG, Leibnizstr. 2, 71032 Böblingen, Germany, lena.michailidis@daimler.com.
Daimler AG, Wilhelm-Runge-Str. 11, 89081 Ulm, Germany, marcus.ziegler@daimler.com.

KINETIC PART–FEEDING MODELS FOR ASSEMBLY LINES IN AUTOMOTIVE INDUSTRIES

MICHAEL HERTY, LENA MICHAILIDIS, AND MARCUS ZIEGLER

Abstract. This paper deals with the modeling of production processes in automotive industries by models based on partial differential equations.The basic idea consists on the derivation of kinetic equations to model production flow on an assembly line. Numerical results based on data of an assembly plant are presented. The work implements a recent discussion [34, 38] for general flow on unstructured networks.
AMS 58F15, 58F17, 53C35
Keywords. Network dynamics, kinetic theory, asymptotic analysis.

1. Introduction

This paper is concerned with the mathematical modeling of high–volume automotive production processes. A new challenge in production is the large variety of different car models produced in almost arbitrary order. Today, the production process needs therefore to be described as high–variant mixed–model assembly lines [28]. We are interested in a mathematical description able to be used for long–term planning of for example workforce capacities, storage capacities and workload predictions. Due to the high volume a discrete mathematical model as for example given by discrete event simulators [7] is challenging to compute for large time periods. It has been argued [2, 3, 4, 22, 38] that models based on partial differential equations are equivalent to discrete event simulations and in particular might be used to describe efficiently the long–term behavior of production processes. Several examples for rigorous derivations of models based on partial differential equations from discrete event simulations exist and we refer to [2, 5] for examples. For an overview on continuous models for production we refer also to [6, 22, 30]. In particular, we refer to [24] for a kinetic model of a production line with priorities and further discussion on the validity of using those equations to describe production processes.

Modeling processes using multi agent approaches have also been employed to study socio-economic problems [1, 20], traffic flow [33, 13] or crowd dynamics [10, 11, 25]. We also refer to [14, 15, 12] for further applications and a general discussion of the derivation of Boltzmann–like equations for complex systems. When modeling the production process we follow an approach recently becoming more popular in the mathematical community. It has been argued that multi agent systems might be used to describe many

Date: June 26, 2014.
RWTH Aachen University, Templergraben 55, 52056 Aachen, Germany, herty@igpm.rwth-aachen.de.
Daimler AG, Leibnizstr. 2, 71032 Böblingen, Germany, lena.michailidis@daimler.com.
Daimler AG, Wilhelm-Runge-Str. 11, 89081 Ulm, Germany, marcus.ziegler@daimler.com.

technical and also biological processes. The arising kinetic and corresponding macroscopic equations may then be analysed to understand pattern formation or long term behavior, see for example [25] for an application to fish and bird swarms. This approach has been fruitful in gas dynamics and has recently been discussed in a general framework including some analysis in [10]. Even so not all areas of application might be well suited for such an approach, see for example the discussion in the modeling of swarms [15], we apply the kinetic approach to production for the following reasons. In order to obtain a meaningful Monte–Carlo game of agents many interactions are required (to allow to neglect history and secondary interactions). Further, the set of rules all agents have to follow is independent of the particular agent. Both assumptions are satisfied for the high–volume production line. The advantage of modeling processes using kinetic equations compared with swarm models for biological simulation lies also precisely in the fact that the car bodies to be assembled are passive and follow a particular set of production rules. This is most likely only some extent in socio–logical or biological models. Needless to say the kinetic approach is only one way to model this phenomena. For an overview of existing approaches we refer to [15] where in the case of swarm modeling different approaches and further references are given.

From a mathematical point of view an automotive assembly line is a graph with products moving along the arcs of this graph. Flows on structured media have been studied widely in the literature in the past years and appear in an almost infinite variety [26, 8, 9, 31, 29, 16]. Here, we will use a similar description of the underlying process as in [34, 38]. In [34] a general production flow problem on a general graph structure has been studied and a kinetic partial differential equation for high–volume part flows is derived. A transport (macroscopic) equation could also be obtained and used as long–time approximation to the kinetic dynamics. Similarly, in [38] a system of hyperbolic equations is derived from a kinetic partial differential equation describing a simple production process on a single line. Statistical information on the production process entered in coefficients of the final hyperbolic equations. In this paper, we discuss results for an assembly line with statistical information obtained by car manufacturing plants. Compared with [38] the underlying particle dynamic is more complicated. In contrast to both references [38, 34] different hyperbolic closure relations are used to derive the macroscopic hyperbolic models. Further, the transport coefficients in the resulting equations are also computed explicitly and include the statistical information available from the manufacturing plant. Further, numerical studies on the macroscopic equation are presented.

2. Mathematical modeling

We are interested in the prediction of the long term behavior of the overall workload within a supply chain, depending on the local statistics of the produced parts at each station, as well as possible variations in production velocity. First, we describe the available data within the production line before turning to the Monte–Carlo description of the process. The kinetic equation is derived also in this section, whereas the macroscopic equations are deduced in the following section 3.

The assembly plant under consideration is located in Germany. All variants of a single type are produced on the same production line within this plant. The production is organized in several steps – a fully automated pre–assembly and manual final production.

At the final production the different possible variants of the car types have to be taken into account. The production is organized along a single line with different stations. Each station represents one production step and each production step requires essentially the assembling of a certain number of parts to a moving car body. However, due to the many variants the number of parts that must be assembled within a fixed station is highly volatile. Historic data on the number of parts is available for a total of $N = 17$ (out of a total of 30) stations from one belt section. Additional statistical data (for example on the production velocity) is available and we comment below on how we use this data.

We model an assembly line therefore by N stations $n = 1, \dots, N$. Due to the high number of variants, we consider a generic car body. The time a car body spends within each station is (currently) fixed and given by $T = 60[sec]$. Within each station n a different number of parts $a(n)$ is assembled to the car body. Due to the many variants this number is not fixed and changes with each arriving car body. From historic data statistical information on the number of parts assembled at each station $a(n)$ is available.

The number of assembled parts for one day and different stations is shown in Figure 1. We use this data to derive a discrete probability distribution function $a \to \mathbf{\Phi}(a, n)$ for each station n. Here, $\mathbf{\Phi}(a, n)$ is the probability to assemble a parts at station n. A typical prediction horizon for car manufacturing is one week whereas the assembly of all parts in the final production step takes one day. Data is available for one week and in order to determine $\mathbf{\Phi}$, we use all available data. In the following it will be advantageous to have a probability function $\Phi(a, n)$ defined for all a. We therefore, interpolate the discrete probability function defined for the values $a_j, j = 1, \dots, M$ by

$$\Phi(a, n) = H(a) \sum_{j=1}^{M} \delta(a - a_j)\mathbf{\Phi}(a_j, n).$$

We have $\Phi(a, n) = 0$ for $a < 0$, Φ is a probability density for each fixed n and H the Heaviside function. The description of the number of assembled parts at each station by a probability density $\Phi(a, n)$ allows to treat all car bodies as non–distinguishable.

So far, a, n are T dimensional quantities. In order to simplify the notation and discussion later on we normalize the quantities by

$$\tilde{a} = \frac{a}{a_0}, \ \tilde{T} = \frac{T}{T_0}$$

where a_0 is the maximal unit of assembled parts overall stations and T_0 the characteristic time of our process being equal to one second. Therefore, from now on $a \in [0, 1]$. We also drop the tilde in the following.

A particle i (resembling a car body) where $i \in \{1, \dots, k \in \mathbb{N}\}$ is moving along the assembly line and has a state X_i. The different stations are called S_n, for $n = 1, \dots N$ and they are in the following considered as nodes in a directed graph. S_1 is the first and S_N the last station in the line. Similar to [34], we assume particles are non–distinguishable. Dimensionless time is denoted by $t \geq 0$. Each particle i has a state $X_i = X_i(t) =$

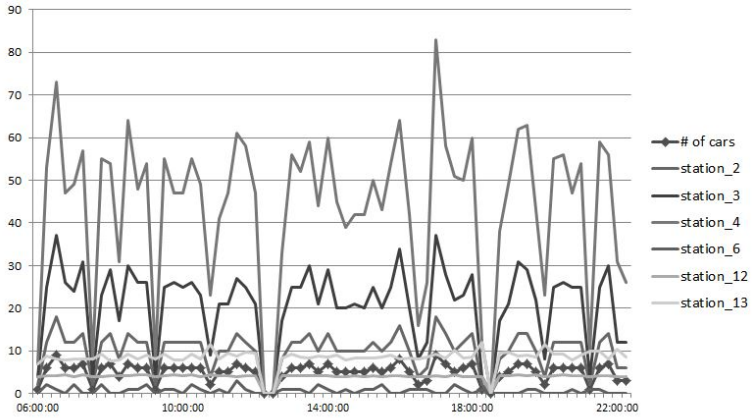

FIGURE 1. Part distributions at different stations along an assembly line over a time period of one day.

$(x(t), \tau(t), a(t), n(t))_i \in \mathbb{R} \times \mathbb{R} \times \mathbb{N} \times \mathbb{N}$ in state space $X = (X_i)_{i=1}^N \subseteq \mathbb{R}^N$ modeling the following: $n_i(t) \in \{1, \dots, N\}$ denotes the station index of particle i at time t. $\tau_i(t) \in \mathbb{R}_0^+$ is the time elapsed within the current station, $a_i(t)$ are the (dimensionless) number of parts assembled to the particle in station $n_i(t)$ and $x_i(t) \in [0, 1]$ is the stage of completion of particle i along the assembly line.

Within a small time interval $\Delta t > 0$ the state of each particle may change according to the following dynamics. If $\tau_i(t) \leq T$ then the particle is in between two stations $n_i(t)$ and $n_i(t) + 1$. Therefore, the number of parts a_i and the station index do not change whereas the elapsed time τ and the stage of completion increases. Note that it is possible, that $\tau_i(t) \geq T$ provided that the state of the particle does not change. The latter is modeled by

$$x_i(t + \Delta t) = x_i(t) + \Delta t \, v(a_i(t)).$$

Theoretically, the stage of completion of the current particle is linear and independent of the number of assembled parts and therefore set the velocity $v \equiv 1$. However, this is not observed in practice where assembly is also conducted outside the designated stations, which means for example that work starts before scheduled time. No model and no data is available to quantify this effect. In order to at least qualitatively asses this problem, we derive a model for a general (sufficiently smooth) function $a \to v(a)$.

Summarizing, we obtain the following dynamics for a particle i and an elapsed time $\tau_i < T$. If $\tau_i(t) \leq T$:

$$\begin{cases} n_i(t + \Delta t) = n_i(t), \; a_i(t + \Delta t) = a_i(t), \\ x_i(t + \Delta t) = x_i(t) + \Delta t \, v(a_i(t)), \; \tau_i(t + \Delta t) = \tau_i(t) + \Delta t. \end{cases} \tag{1}$$

When $\tau_i(t) \geq T$ the particle has arrived at the next station. Here, it will change state due to the fact that a new number of assembled parts is assigned. Within any time interval Δt the change of state upon arrival happens with probability $\omega \Delta t$, where ω is the so–called collision frequency. In the considered assembly line this frequency is $\omega = \frac{1}{T}$, however, in order to discuss more general models, we keep the general variable $\omega > 0$. If

the particle changes state the new number of parts α is obtained by random sampling from the probability distribution $\Phi(a, n_i(t)+1)$, i.e., $dP(\alpha = s) = \Phi(s, n_i(t)+1)ds$. We also increase the stage of completion and reset the elapsed time τ_i to zero. Hence, we obtain the dynamics for the particle i. If $\tau_i(t) \geq T$:

$$
\begin{cases} n_i(t+\Delta t) = n_i(t)(1-\omega\Delta t) + (n_i(t)+1)\omega\Delta t, \\ a_i(t+\Delta t) = a_i(t)(1-\omega\Delta t) + \alpha\omega\Delta t, \ P(\alpha = s) = \Phi(s, n_i(t)+1), \\ x_i(t+\Delta t) = x_i(t) + \Delta t\ v(a_i(t)), \ \tau_i(t+\Delta t) = (\tau_i(t)+\Delta t)(1-\omega\Delta t). \end{cases} \tag{2}
$$

Denoting by $s \to H(s)$ the Heaviside function, we restate the previous dynamics for particle i as

$$
\begin{cases} x_i(t+\Delta t) = x_i(t) + \Delta t v(a_i(t)), \\ n_i(t+\Delta t) = n_i(t)H(T-\tau_i(t)) + H(\tau_i(t)-T)\left((1-\omega\Delta t)n_i(t) + \omega\Delta t(n_i(t)+1)\right), \\ a_i(t+\Delta t) = a_i(t)H(T-\tau_i(t)) + H(\tau_i(t)-T)\left((1-\omega\Delta t)a_i(t) + \omega\Delta t\alpha\right), \\ \tau_i(t+\Delta t) = (\tau_i(t)+\Delta t)\,H(T-\tau_i(t)) + H(\tau_i(t)-T)\left((1-\omega\Delta t)(\tau_i(t)+\Delta t)\right). \end{cases} \tag{3}
$$

Under molecular chaos assumption a kinetic equation for the single particle probability density $f(t, X)$ with $X = (x, \tau, a, n)$ is derived. Here, we denote by $f(t, X)dX$ the probability to find a particle in state X at time t. Since (x, τ, a) are continuous states but n is discrete we have that

$$
\frac{1}{N}\sum_{n=1}^{N}\int f(t, X)dxd\tau a = 1. \tag{4}
$$

The derivation of the equation for the single particle density is a straight–forward but lengthy computation. Therefore the details are given in the appendix A, in particular they are given by equations (40) and (46) depending on whether the change of state is reversible or not. We observe that the dynamics (3) is composed of three exclusive events appearing with state–dependent probabilities $\beta_1 = H(T-\tau)$, $\beta_2 = H(\tau-T)\omega\Delta t$ and $\beta_3 = H(\tau-T)(1-\omega\Delta t)$ since $\sum_{i=1}^{3}\beta_i = 1$. Herein, events related to β_1 and β_2 are reversible changes of the state X. Therefore, the probability density $f(t, X)$ evolves in case of those events according to equation (40). In the case of an event related to β_3 the new state is $\tau = 0$. This is a non–invertible dynamics and we obtain a term similar to equation (46). Therefore, f fulfills the following time–discrete equation

$$
\begin{aligned} f(t+\Delta t, X) &= H(T-\tau+\Delta t)f(t, x-\Delta t v(a), \tau-\Delta t, a, n) \\ &\quad + H(\tau-\Delta t-T)(1-\omega\Delta t)f(t, x-\Delta t v(a), \tau-\Delta t, a, n) \\ &\quad + \omega\Delta t\Phi(a, n)\delta(\tau)\int f(t, x-\Delta t v(\bar{a}), \bar{\tau}, \bar{a}, n-1)H(\bar{\tau}-T)d\bar{\tau}d\bar{a}. \end{aligned} \tag{5}
$$

Provided f fulfills equation (4) at time t, also

$$
\sum_{n=1}^{N}\int f(t+\Delta t, X)dxd\tau da \ = \ 1
$$

holds.

A formal Taylor expansion shows that the differential form of the previous equation is

$$\partial_t f(t,x,\tau,a,n) + \partial_x(v(a)f(t,x,\tau,a,n)) = C(f) \tag{6}$$

and a collision operator

$$C(f) = -\partial_\tau f - \omega H(\tau - T)f + \omega\Phi(a,n)\delta(\tau)\int f(x,\bar\tau,\bar a,n-1)H(\bar\tau - T)d\bar\tau d\bar a. \tag{7}$$

If not stated otherwise the integration in the collision operator is on the full domain. It remains to discuss the case $n = 1$. In the following, we study a *periodic problem*, i.e., we assume that the last station $n = N$ is equivalent to station $n = 0$ and have $f(t,x,\tau,a,0) := f(t,x,\tau,a,N)$. Then, equation (6)-(7) is well–posed for all $n = 1,\dots,N$.

Alternatively, one would need to prescribe boundary data for $n = 1$. The equation (6) is a high–dimensional kinetic equation on the phase space X. A full discretization is therefore computationally expensive. As in gas dynamics [17] or in production models [38, 34], we therefore derive approximate, low–dimensional (macroscopic) models, capturing some qualitative properties of the kinetic dynamics in section 3. In order to do so, we proceed as in gas dynamics [18, 38, 17].

To this end, we first analyse the kernel of $C(f)$. The analysis is similar to [34], however, there are some differences due to the different particle dynamics. As in [34] the kernel of C is decomposed in an invertible and non–invertible part similar to the previously given dynamics.

Lemma 2.1. *The kernel $C(f)$ (7) is decomposed as $C(f) = B(D(f))$ where*

$$\begin{cases} D(f) &= \partial_\tau f + \omega H(\tau - T)f, \\ B(f) &= \Phi(a,n)\delta(\tau)\int f(x,\bar\tau,\bar a,n-1)d\bar a d\bar\tau - f. \end{cases} \tag{8}$$

For a proof of this lemma it suffices to note that for integrable functions f, we have $\int \partial_\tau f d\tau = 0$.

The kernel manifold of $C(f)$ is computed as the kernel of $B(f)$. We obtain

$$f(t,x,\tau,a,n) = \frac{1}{T + \frac{1}{\omega}}\delta(\tau)\Phi(a,n)\rho(t,x) \ \in ker(B), \tag{9}$$

for any product density function $\rho(t,x)$ which is defined later on. This is due to the fact that $C(f)$ is not acting on time t and space x. Therefore, any steady state solution may be multiplied by a factor $\rho(t,x)$. The additional factor $\frac{1}{T+\frac{1}{\omega}}$ is used to simplify the computations later on. Obviously, it is not necessary and may be incorporated in $\rho(t,x)$. Note that depending on $\rho(t,x)$ f is not necessarily a probability density.

In order to obtain the kernel of C, we compute the inverse of the operator D and solve for general $\rho(t,x)$ equation

$$\partial_\tau f + \omega H(\tau - T)f = \frac{1}{T + \frac{1}{\omega}}\delta(\tau)\Phi(a,n)\rho(t,x). \tag{10}$$

The solution (in the weak sense) of the previous equation with initial data $f(\tau = -\infty) = 0$ is

$$f(t,x,\tau,a,n) = \frac{1}{T+\frac{1}{\omega}}\Phi(a,n)\rho(t,x)\begin{pmatrix} 0 & \tau \leq 0 \\ 1 & 0 < \tau \leq T \\ \exp\left(-\omega(\tau - T)\right) & \tau \geq T \end{pmatrix} \tag{11}$$

We remark that the solution f in (11) is discontinuous at $\tau = 0$ leading to the δ distribution as derivative (in the sense of distributions). At $\tau = T$ the solution is continuous and equation (10) is fulfilled in the integral sense. A sketch of f is given in Figure 2 for $\rho \equiv 1$.

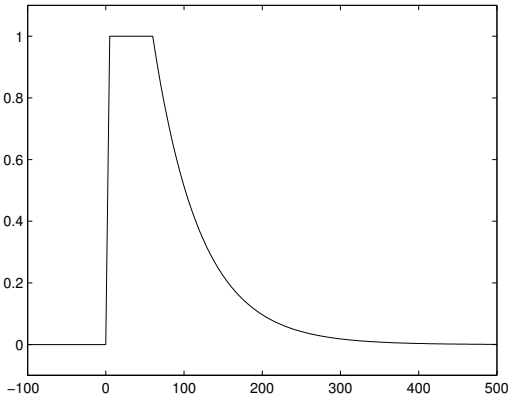

FIGURE 2. Sketch of the solution $\tau \to f(t,x,\tau,a,n)$ for fixed (t,x,a,n) given by equation (11) with $T = 100$, $\omega = 1$ and $\Phi \equiv \rho \equiv 1$.

We are interested in solutions f to equation (6) that are probability distributions. Hence, among the family of solutions in the kernel of C given by (11) we are only interested in solutions fulfilling equation (4). Choosing $\rho(t,x)$ as in equation (12) we obtain the desired steady–states. This leads to the definition of the mass density of our system as

$$\rho(t,x) := \frac{1}{N}\sum_{n=1}^{N}\int f(t,x,\tau,a,n)dad\tau. \tag{12}$$

This definition of ρ may also be used out of steady–state. We are now interested in an evolution equation for ρ independent of knowledge on f. Such an equation may be derived using different approaches.

Using the definition (12) we consider the following projection [38]. Let f be any solution to (6). Then, Pf projects f onto the kernel of C. Pf is defined using the

explicit representation (11), i.e.,

(13)
$$Pf = \frac{1}{T+\frac{1}{\omega}}\Phi(a,n)\begin{pmatrix} 0 & \tau \le 0 \\ 1 & 0 < \tau \le T \\ \exp\left(-\omega(\tau - T)\right) & \tau \ge T \end{pmatrix}\left(\frac{1}{N}\sum_{n=1}^{N}\int f(t,x,\tau,a,n)dad\tau\right)$$

and write

$$f = Pf + (1-P)f. \tag{14}$$

Using the periodicity in the stations it is easy to see that $P(\partial_t f) = \partial_t Pf$ and $PC(f) = C(P(f)) = 0$. Applying the projection P to the kinetic equation (6), summation on n and integration on a and τ yields

$$\begin{cases} \partial_t \rho(t,x) + \partial_x\left(\varphi\rho(t,x)\right) + \partial_x\psi = 0, \\ \varphi(a,n) = \frac{1}{N}\sum_{n=1}^{N}\int v(a)\Phi(a,n)da, \\ \psi(t,x,\tau,a,n) = \frac{1}{N}\sum_{n=1}^{N}\int v(a)(1-P)f dad\tau. \end{cases} \tag{15}$$

The previous equation arises due to the following equivalence

$$\frac{1}{N}\sum_{n=1}^{N}\int P(\partial_t f(t,x,\tau,a,n))dad\tau = \partial_t\rho(t,x), \tag{16}$$

and since

$$\begin{aligned} &\frac{1}{N}\sum_{n=1}^{N}\int P\Big(\partial_x v(a) f(t,x,\tau,a,n)\Big)dad\tau \\ &= \partial_x\Big\{\frac{1}{N}\sum_{n=1}^{N}\int \Phi(a,n)\frac{1}{T+\frac{1}{\omega}}\begin{pmatrix} 0 & \tau \le 0 \\ 1 & 0 < \tau \le T \\ \exp\left(-\omega(\tau - T)\right) & \tau \ge T \end{pmatrix} dad\tau \\ &\times\left(\frac{1}{N}\sum_{n=1}^{N}\int v(a) f(t,x,\tau,a,n)d\tau da\right)\Big\} \\ &= \partial_x\left(\frac{1}{N}\sum_{n=1}^{N}\int v(a)\left(Pf + (1-P)f\right)(t,x,\tau,a,n)d\tau da\right) \\ &= \partial_x\left(\frac{1}{N}\sum_{n=1}^{N}\int v(a)\Phi(a,n)da\,\rho(t,x)\right) + \partial_x\left(\frac{1}{N}\sum_{n=1}^{N}\int v(a)(1-P)f d\tau da\right). \end{aligned} \tag{17}$$

Equation (15) propagates the density with the expected value of $v(a)$ with respect to the probabilities $\Phi(a,n)$. Using $\mathbb{E}_\Phi$ to denote the expectation with respect to the probability density Φ and by $\mathbf{E}$ the sum of the expectations, we may rewrite φ as

$$\varphi = \frac{1}{N}\sum_{n=1}^{N}\mathbb{E}_{\Phi(\cdot,n)}(v) = \mathbf{E}(v) \tag{18}$$

For general functions $v(a)$ equation (15) is not in a closed form for ρ and we discuss closure relations in the following section 3.

3. Macroscopic equations

In this section, we derive the macroscopic approximations for solutions f to (6)-(7). We first discuss possible closure relations for equation (15). Different approaches are known in the literature to derive a closed form. As already observed in [38] the classical Chapman–Enskog expansion [17] yields a parabolic model for the evolution of the density ρ. This however has the drawback of infinite speed of propagation of waves which is undesirable in the context of assembly lines. Therefore, we aim in deriving partial differential equations allowing for finite speed of propagation . Since furthermore the total number of particles should remain constant we have a conservation property of our equation for the total mass $\int \rho(t,x)dx$. Therefore, we use a moment approximation to obtain a hyperbolic system of conservation laws for the evolution of ρ. Here, hyperbolicity of the partial differential equation is defined as in [21].

3.1. Asymptotic expansion.

If we are interested in the qualitative long–time behavior of f, then we may rescale time and space by $t \to t/\epsilon$ and $x \to x/\epsilon$ for some small positive value of ϵ. Using this hyperbolic scaling and denoting the new variables again as (t,x), we obtain $\partial_t f + \partial_x v f = \frac{1}{\epsilon} C(f)$. Expanding f in terms of ϵ, we obtain as order $O(1)$ approximation f^0 which is given by equation (11) and where $\rho(t,x)$ fulfills equation (15). We review approaches to close equation (15). The scaling approach makes use of dimensionless quantities.

The case $v(a) = cst$. In the case $v(a)$ constant the equation (15) simplifies and we have $\varphi = cst$ and $\psi = 0$. Therefore, ρ is simply transported with speed equal to one and no closure relation is required. In the following, we assume v is not constant.

Chapman–Enskog inspired ansatz. A closure relation has been suggested in [38] and we briefly apply the procedure to the current system. Since C is linear in f, equation (19) for $\sigma = (1-P)f$ obtained from the rescaled kinetic equation reads

$$\partial_t \sigma + (1-P)\partial_x (v\sigma) = \frac{1}{\epsilon} C(\sigma). \tag{19}$$

and we have

$$\psi = \frac{1}{N} \sum_{n=1}^{N} \int v\sigma d\tau da.$$

The system (15),(19) is still not in closed form. Therefore, in [38] it has been assumed that the approximation (20) for σ similar to equation (11) holds true. Let σ be given by

$$\sigma(t,x,\tau,a,n) = j(t,x)S(\tau,a,n), \qquad \frac{1}{N}\sum_{n=1}^{N} \int aS(\tau,a,n)d\tau da = 1. \tag{20}$$

Due to equation (20) the system (ρ, j) fulfills

$$\partial_t \begin{pmatrix} \rho(t,x) \\ j(t,x) \end{pmatrix} + \partial_x A \begin{pmatrix} \rho(t,x) \\ j(t,x) \end{pmatrix} = \begin{pmatrix} 0 \\ j(t,x)\frac{1}{N} \sum\limits_{n=1}^{N} \int a \frac{1}{\epsilon} C(S) d\tau da \end{pmatrix}, \tag{21}$$

where

(22)
$$A = \frac{1}{N}\sum_{n=1}^{N}\begin{pmatrix} \int v(a)\Phi(a,n)da & \int v(a)Sd\tau da \\ 0 & \int av(a)Sd\tau da - \int a\Phi(a,n)da\frac{1}{N}\sum\limits_{m=1}^{N}\int v(a)Sd\tau da \end{pmatrix}$$

The previous system is still not closed since $S = S(\tau, a, n)$ is unknown. In [38] the shape of S has been determined by comparing the solution with a classical Chapman–Enskog expansion. Since this leads to an asymptotic expansion in ϵ to Chapman–Enskog like model, we do not pursue this direction here. For further details, we refer to [38, page 8].

3.2. **Moment approximations.** In order to derive new equations, we pursue an approach based on the kinetic equation (6) and use a moment approximation in the assembled parts a [27, 36]. As before we consider mass density as in (12),

$$\rho(t,x) := \frac{1}{N}\sum_{n=1}^{N}\int f(t,x,\tau,a,n)d\tau da.$$

Since the kernel $C(f)$ conserves mass, we obtain by integration of (6) equation (15).

Instead of a projection to the kernel manifold, we derive an equation for the first moment (ρu)

$$(\rho u)(t,x) := \frac{1}{N}\sum_{n=1}^{N}\int v(a)f(t,x,\tau,a,n)d\tau da. \tag{23}$$

We obtain

$$\begin{aligned} &\partial_t(\rho u(t,x)) + \partial_x \frac{1}{N}\sum_{n=1}^{N}\int v^2(a)f(t,x,\tau,a,n)d\tau da \\ &= \omega\frac{1}{N}\sum_{n=1}^{N}\int \mathbb{E}_{\Phi(\cdot,n)}(v)H(\tau - T)f(t,x,\tau,a,n-1) \\ &- v(a)H(\tau - T)f(t,x,\tau,a,n)d\tau da \end{aligned} \tag{24}$$

In resemblance of gas dynamics, we may rewrite the previous equation as

$$\begin{aligned} &\partial_t(\rho u) + \partial_x\left(p[f] + \rho u^2\right) = Q[f], \text{ with} \\ &p[f] = \frac{1}{N}\sum_{n=1}^{N}\int (v-u)^2 f d\tau da, \text{ and} \\ &Q[f] = \omega\frac{1}{N}\sum_{n=1}^{N}\int \mathbb{E}_{\Phi(\cdot,n)}(v)H(\tau - T)f(t,x,a,n-1,\tau) \\ &\quad -v(a)H(\tau - T)f(t,x,a,n,\tau)d\tau da. \end{aligned} \tag{25}$$

Note that in the case $v(a) = cst$, we have $u(t,x) = cst\rho(t,x)$ and we obtain the same equation as in section 3.1, i.e., equation (15) with $\varphi = cst$ and $\psi \equiv 0$.

Next, we discuss different closure relations to approximate $Q[f]$ and $p[f]$. Note that in all cases, the equations are given by

$$\begin{cases} \partial_t \rho + \partial_x(\rho u) & = 0, \\ \partial_t(\rho u) + \partial_x(\rho u^2 + p[f]) & = Q[f]. \end{cases} \tag{26}$$

Define for the following discussion the projection f^{eq} as projection onto the kernel.

$$f^{eq}(t,x,\tau,a,n) := \frac{1}{T+\frac{1}{\omega}}\Phi(a,n)\begin{pmatrix} 0 & \tau \le 0 \\ 1 & 0 < \tau \le T \\ \exp\left(-\omega(\tau - T)\right) & \tau \ge T \end{pmatrix}\rho(t,x) \tag{27}$$

Note that the following is precisely Pf, but now we choose to rewrite the mass density relation in terms of ρ in order to obtain a closed formula. The function $f^{eq}(t,x,\tau,a,n)$ then fulfills for all fixed t the steady–state equation $C(f) = 0$.

Hence, replacing in p and Q the general f by f^{eq} leads to a closed system of equations for ρ and ρu. From a modeling point of view this implies that in p and Q only variations on the steady–state manifold are considered. Therefore, p and Q are approximated by its action on variation within the kernel.

However, we may not simply replace (p, Q) by $(p[f^{eq}], Q[f^{eq}])$. By definition of the projection operator Pf we have that

$$\frac{1}{N}\sum_{i=1}^{N}\int f^{eq}(t,x,\tau,a,n)d\tau da = \rho(t,x)$$

and

$$\frac{1}{N}\sum_{i=1}^{N}\int v(a) f^{eq}(t,x,\tau,a,n)d\tau da = \mathbf{E}(v(\cdot))\rho(t,x).$$

Hence, similar to traffic flow [35], the collision operator only preserves the density but *not* the first moment (ρu). Therefore, closing equations (26) by setting $(p, Q) = (p[f^{eq}], Q[f^{eq}])$ is not well–defined.

In the following we therefore investigate *other* approaches to close the equation (26) using the idea to replace (p, Q) by $(p[f^{eq}], Q[f^{eq}])$ but for f^{eq} such that the moments ρ and (ρu) are preserved for f^{eq}. We refer for example to [27, 36] for additional possibilities not discussed here.

3.2.1. *Monokinetic closure.* Assume $v(a)$ is strictly monotone. Then, we may close the system using a monokinetic distribution function [23, 1]. To this end define the equilibrium function

$$f^{eq}(t,x,\tau,a,n) := \rho(t,x)\delta(\tau)\delta(v(a) - u)v'(a).$$

One verifies easily that for

$$\frac{1}{N}\sum_{n=1}^{N}\int f^{eq}d\tau da = \rho(t,x) \text{ and } \frac{1}{N}\sum_{n=1}^{N}\int v(a) f^{eq}d\tau da = (\rho u)(t,x) \tag{28}$$

the moments are conserved. Replacing now the pressure and source term yields the corresponding approximations

$$p[f^{eq}] = 0,\ Q[f^{eq}] = 0, \tag{29}$$

so that the resulting system (26) coincides with system of pressureless gas dynamics.

Since the equations are independent of $\Phi(a,n)$ no statistical information of the assembly line enters. Further, the closure implies that essentially all cars are concentrated at zero elapsed time and traveling with the velocity of the ensemble.

3.2.2. *Extended equilibrium function.* Based on the deterministic data from Section 2 and carrying on with a continuous solution, we are interested in a closure relation which represents the deterministic problem from the beginning. Therefore, we apply a Grad closure procedure. An extended equilibrium function is constructed for example using the Grad closure. We define for given ρ and u set

$$f^{eq}(t,x,\tau,n) := \frac{1}{T+\frac{1}{\omega}}\Phi(a,n)\begin{pmatrix} 0 & \tau \le 0 \\ 1 & 0<\tau\le T \\ \exp\left(-\omega(\tau-T)\right) & \tau \ge T \end{pmatrix} \rho(t,x)\left(\lambda_0+\lambda_1 v(a)\right).$$

Herein, λ_0, λ_1 are functions depending on ρ and u. Using the moment relations we obtain the following set of equations determining (λ_0,λ_1) :

$$\begin{cases} \rho(t,x)\left(\lambda_0+\lambda_1 \mathbf{E}(v(\cdot))\right) & = \rho(t,x), \\ \rho(t,x)\left(\lambda_0 \mathbf{E}(v(\cdot)) + \lambda_1 \mathbf{E}(v^2(\cdot))\right) & = \rho(t,x)u(t,x). \end{cases} \tag{30}$$

Recall the notation of (18) where $\mathbf{E}(g) = \frac{1}{N}\sum_{n=1}^{N} \mathbb{E}_{\Phi(\cdot,n)}(g(\cdot))$. Also, we denote by $\mathbf{V}(v) = \mathbf{E}(v^2) - \mathbf{E}(v)^2$. The previous system is solved for (λ_0,λ_1) provided that $\mathbf{V}(v)$ is non–zero (which excludes in particular the case $v(a) = cst$) as

$$\lambda_0(u) = \frac{\mathbf{E}(v^2) - u\mathbf{E}(v)}{\mathbf{V}(v)},\ \lambda_1(u) = \frac{u-\mathbf{E}(v)}{\mathbf{V}(v)}.$$

Hence, we may close (26) by evaluating p and Q at the extended equilibrium function f^{eq}. The function f^{eq} for the previously computed choice of λ_0 and λ_1 then has the moments ρ and ρu.

$$\begin{aligned} p[f^{eq}] &= \frac{1}{N}\sum_{n=1}^{N}\int (v(a)-u)^2 P f\left(\lambda_0(u)+\lambda_1(u)v(a)\right) d\tau da \\ &= \rho\lambda_0(u)\left(\mathbb{E}(v^2) - 2u\mathbb{E}(v) + u^2\right) + \rho\lambda_1(u)\left(\mathbb{E}(v^3) - 2\mathbb{E}(v^2)u + \mathbb{E}(v)u^2\right) \\ &= -\rho u^2 + \frac{\rho\left(\mathbb{E}^2(v^2) - \mathbb{E}(v^3)\mathbb{E}(v)\right) + \rho u\left(\mathbb{E}(v^3) - \mathbb{E}(v)\mathbb{E}(v^2)\right)}{\mathbf{V}(v)}. \end{aligned} \tag{31}$$

$$
\begin{aligned}
(32)\qquad Q[f^{eq}] &= \omega \frac{1}{N} \sum_{n=1}^{N} \int \Big(\mathbb{E}_{\Phi(\cdot,n)}(v) P f(t,x,a,n-1,\tau) \\
&\quad - v(a) P f(t,x,a,n,\tau) \Big) H(\tau - T)(\lambda_0(u) + \lambda_1(u) v(a)) d\tau da \\
&= \frac{\rho \lambda_0(u)}{T + \frac{1}{\omega}} \left(\frac{1}{N} \sum_{n=1}^{N} \mathbb{E}_{\Phi(\cdot,n)}(v) - \mathbb{E}(v) \right) \\
&\quad + \frac{\rho \lambda_1(u)}{T + \frac{1}{\omega}} \left(\frac{1}{N} \sum_{n=1}^{N} \mathbb{E}_{\Phi(\cdot,n)}(v) \mathbb{E}_{\Phi(\cdot,n-1)}(v) - \mathbb{E}(v^2) \right) \\
&= \frac{\rho u - \rho \mathbb{E}(v)}{\mathbf{V}(\mathbf{v})(T + \frac{1}{\omega})} \left(\frac{1}{N} \sum_{n=1}^{N} \mathbb{E}_{\Phi(\cdot,n)}(v) \mathbb{E}_{\Phi(\cdot,n-1)}(v) - \mathbb{E}(v^2) \right).
\end{aligned}
$$

Summarizing, we obtain the following system for the evolution of $(\rho, \rho u)$

$$
(33)\qquad \begin{cases} \partial_t \rho + \partial_x(\rho u) & = 0, \\ \partial_t(\rho u) + \partial_x(\rho c_1 + (\rho u) c_2) & = (\rho u) c_3 + \rho c_4. \end{cases}
$$

The constants c_i depend on the statistical information of $\Phi(a,n)$ and are given by

$$
(34)\qquad \begin{cases} c_1 \mathbf{V}(v) & = \mathbb{E}^2(v^2) - \mathbb{E}(v^3)\mathbb{E}(v), \\ c_2 \mathbf{V}(v) & = \mathbb{E}(v^3) - \mathbb{E}(v)\mathbb{E}(v^2), \\ c_3 \mathbf{V}(v)(T + \frac{1}{\omega}) & = \frac{1}{N} \sum\limits_{n=1}^{N} \mathbb{E}_{\Phi(\cdot,n)}(v) \mathbb{E}_{\Phi(\cdot,n-1)}(v) - \mathbb{E}(v^2), \\ c_4 & = -\mathbb{E}(v) c_3. \end{cases}
$$

The density $\rho(t,x)$ is the (station-)averaged number of parts at production stage $x \in (0,1)$ and we are interested in the time–evolution of this quantity.

The system (33) is a linear hyperbolic balance law provided that the hyperbolicity property $4c_1 + c_2^2 > 0$ holds. In this case the real eigenvalues are

$$
(35)\qquad \lambda_{1,2} = \frac{c_2}{2} \Psi \frac{1}{2} \sqrt{4c_1 + c_2^2}
$$

and there exists a full set of eigenvectors. If we assume, that all probability density functions are equal $\Phi(a,n) = \Psi(a)$ then the Grad closure Ansatz is well–defined provided that the variance is non–zero. This also implies that $\mathbf{V}(v) > 0$. In section 4, we numerically compute $\lambda_{1,2}$ for the available statistical data. Further, in the example of an assembly line, we have $\Phi(a,n) = 0$ for $a < 0$ and therefore all moments (36) are non–negative $E_n^i \geq 0$. It turns out that also in this case the eigenvales are real and $\mathbf{V}(v) > 0$. Since also the source terms are linear an initial value problem for equation (33) is well–posed. This result has been established in a more general setting for example in [19]. Note that the model (33) may as well produce negative values for ρ due to the presence of the source term in the equation for (ρu).

In the following remark, we give an example of the arising coefficients in a simplified setting. The real data will be considered in the following section.

Remark 3.1. *The velocity $v(a)$ describes the speed at which parts are assembled to the car body. This speed depends on the number of parts to be mounted. So far, we do not have data on this function. However, it seems reasonable to assume that $v(a)$ is at least monotone decreasing in the number of mounted parts. The simplest model is linear and therefore would be similar to the speed-density relationship from Greenshields velocity model [32]:*

$$v(a) = 1 - a,$$

Observe that the number of parts has been normalized to one. Let E_n^i be the ith moment of the probability density $a \to \Phi(a, n)$, i.e.,

$$E_n^i = \int a^i \Phi(a, n) da. \tag{36}$$

Then, we obtain the following equations

$$\mathbb{E}(v) = 1 - \frac{1}{N}\sum_{n=1}^{N} E_n^1, \quad \mathbb{E}(v^2) = 1 + \frac{1}{N}\sum_{n=1}^{N} E_n^2 - 2E_n^1,$$

$$\mathbb{E}(v^3) = 1 + \frac{1}{N}\sum_{n=1}^{N}(-3E_n^1) + 3E_n^2 - E_n^3, \quad \mathbf{V}(v) = \frac{1}{N}\sum_{n=1}^{N} E_n^2 - \left(\frac{1}{N}\sum_{n=1}^{N} E_n^1\right)^2,$$

$$\frac{1}{N}\sum_{n=1}^{N} \mathbb{E}_{\Phi(\cdot,n)}(v)\mathbb{E}_{\Phi(\cdot,n-1)}(v) = 1 + \frac{1}{N}\sum_{n=1}^{N} E_n^1 E_{n-1}^1 - 2E_n^1.$$

Note that for the last equation, we used the periodicity assumption $\Phi(a, 0) \equiv \Phi(a, N)$. If we additionally assume, that $\Phi(a, n) = \Psi(a)$ and $\Psi(a) = 2H(a)\psi(a)$ where $\psi(a) = \frac{1}{\sqrt{2\pi}}\exp(-\frac{x^2}{2})$ is the probability density of the normal distribution with mean $\mu = 0$ and variance $\sigma^2 = 1$. Then, we obtain $E_n^1 = \sqrt{\frac{2}{\pi}}$, $E_n^2 = 1$, $E_n^3 = 2E_n^1$ and therefore

$$\mathbb{E}(v) = 1 - \sqrt{\frac{2}{\pi}},\ \mathbb{E}(v^2) = 2\mathbb{E}(v),\ \mathbb{E}(v^3) = 4 - 5E_n^1,\ \mathbf{V}(v) = 1 - \frac{2}{\pi} > 0,$$

$$(\mathbb{E}(v))^2 = \frac{1}{N}\sum_{n=1}^{N} \mathbb{E}_{\Phi(\cdot,n)}(v)\mathbb{E}_{\Phi(\cdot,n-1)}(v),$$

$$c_1\mathbf{V}(v) = (1 - E_n^1)E_n^1 > 0,\ c_2\mathbf{V}(v) = 2 - E_n^1 - 2(E_n^1)^2 \neq 0.$$

Hence, in this case both eigenvalues (35) are real and separate leading to a hyperbolic balance equation (33).

4. Statistical information on the assembly line

For a production plant of a factory, statistical information has been collected along the final assembly line. We present in the following diagram distribution probabilities $a \to \Phi(a, n)$ of assembled parts within different stations n along the assembly line. The probability density $\Phi(a, n)$ at eight selected stations n (out of 17) is depicted in Figure

3. As described in the introduction, the data has been collected by using a daily average of the number of parts at each station. We use historic data from a one week production cycle.

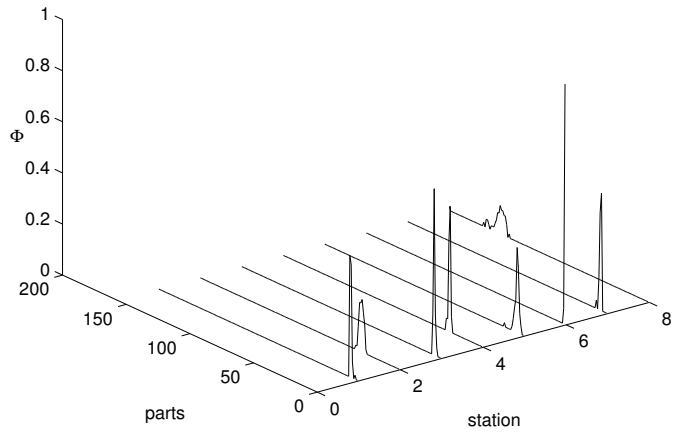

FIGURE 3. Statistical information available along the assembly line at eight selected stations.

Furthermore, we present results on the dependence of φ given by equation (18) on the transport velocity $v(\cdot)$. Currently, the assumption is that the assembly line runs independent of a. However, it is observed in practice that the production within some stations n is not completed within T leading to congestion and possibly highly utilized stations. We illustrate this in Figure 4 where the utilization of the assembly line and the utilization or load of each station is shown. This figure is obtained from the same data on the production line as above. We observe a huge difference between over- and underload. Figure 4 depicts the workload and the degree of capacity at stations. The degree of capacity is separated into three parts: under 95%, between 95% and 100% and over 100%. This effect will be included in the presented model by using a non constant velocity function $v(a)$.

This motivates the assumption, that a constant velocity $v(a)$ independent of the number of parts is *not* realistic. We consider the extended equilibrium function and based on the available statistical data, we compute the transport coefficients in equation (33). We set $T = 60[sec]$ and $\omega = 1/T$. The maximal number of assembled parts is $a_{\max} = 200$. In the following, we investigate different models for transport velocities and compute the hyperbolicity property as well as the coefficients c_i for $i = 1, \dots, 4$. The simplest possible choice (37) is a Greenshields like model [32] with slope $0 < \kappa < 1$.

$$v(a) = 1 - \kappa \frac{a}{a_{\max}} \tag{37}$$

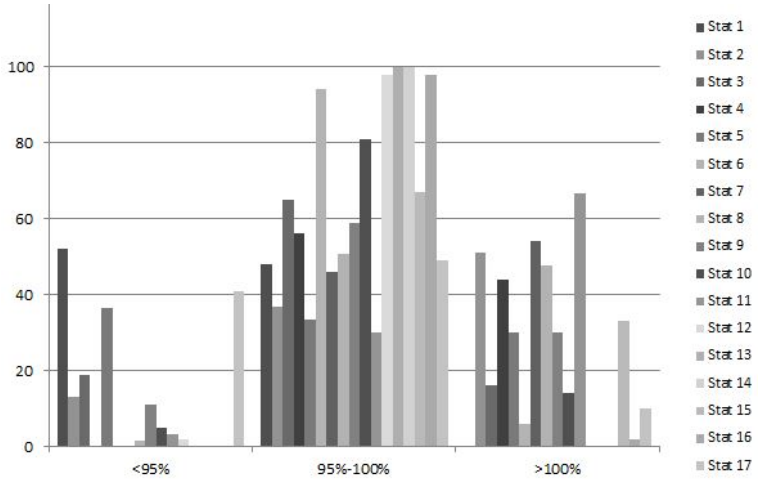

FIGURE 4. Degree of capacity utilization at selected stations

Alternatively, we also consider below a velocity model given by

$$v(a) = 2 - \exp(\kappa \frac{a}{a_{\max}}). \tag{38}$$

For the given data $\Phi(a, n)$, we present in Figure 5 and Figure 6 the value of the coefficients $c_1, \dots, c_4$, $\mathbb{E}(v), \mathbb{E}(v^2)$ and $\mathbb{E}(v^3)$ for the choices of $v(a)$. We observe that for all κ the eigenvalues (35) are real and $\mathbf{V}(v) > 0$. We therefore numerically discretize the linear transport equations (33) by standard first-order finite volume and operator splitting to treat the source term. Therefore, an Upwind scheme combined with an implicit discretization in time of the source term has been applied. This is certainly only one possibility to discretize the preceding equations. Due to the one–dimensionality of the problem we may use very high number of grid points and even be computationally efficient. All numerical results are obtained on an equidistant grid $x \in [0, 1]$ with $N_x = 400$ discretization points and Δt such that the CFL (Courant-Friedrichs-Lewy) condition is fulfilled. In order to simulate the time evolution of the density $\rho(t, x)$, we need to prescribe an initial station-averaged car distribution $\rho(t = 0, x)$. As initial data for $(\rho u)(t = 0, x)$, we consider the definition (24) and replace f by Pf and density $\rho(t = 0, x)$. With this choice and if we prescribe a constant car distribution $\rho(t, x = 0) = \rho_o$, then $(\rho u)(t, 0) = (\rho u)_o$ is constant.The eigenvalues $\lambda_{1,2}$ of (33) for different values of κ are depicted in Figure 7. They are positive and between $\approx \frac{1}{2}$ and one in all cases. Therefore, any perturbation of the state ρ_o will be transported towards $x = 1$. Hence, the total simulation time can be limited to $T = 120$. Assuming similar assembly times for each part, we study a production line at $\rho_0 = 95\%$ load and a perturbation of 0.1%. We prescribe a small perturbation at $x = 1\%$ as $\rho(t = 0, x) = \rho_o - 0.1\% \ \exp(-(8x)^2)$. This leads to a perturbation in density and flow.

The coefficients c_3 and c_4 exceed the order of the coefficients of c_1 and c_2 by at least one order. Therefore, the dynamics are mainly driven by the exponential growth of (ρu) over time. This might lead to an increase or decrease in density. The model itself has no mechanism to prevent densities larger than one or less than zero. Therefore, we simulate

(33) until time t^* where at one stage of completion x^* either the car density exceeds one. In Figure 9, we show the degree of completion x^* at which the initial perturbation has lead to a density exceeding one. We repeat the experiment under a smaller load of the assembly line, namely, $\rho_o = 70\%$, and for a perturbation located at $x = 25\%$ and present the corresponding results in Figure 9. We observe that in this case for $\kappa = 0.9$ and (38) the density did not exceed one within the given time interval.

The typical load of an assembly line is $\rho_o = 95\%$. We now compare Figure 4 and Figure 8 in order to estimate the unknown parameter κ. In Figure 4, we observe, that at 13 out of 17 stations there is production density observed, which is larger than the (desired) maximal load. The station averaged capacity utilization is between 20% and 40% for those stations. Identifying the capacity utilization with degree of completion (x) and assuming the initial perturbation is at position 1%, we observe that for both velocity models a suitable value for $\kappa \in (0.3, 0.6)$.

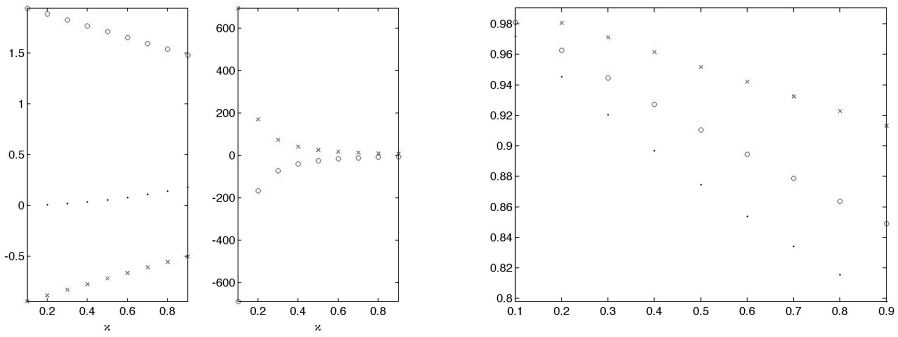

FIGURE 5. Transport coefficients $c_1, \ldots, c_4$ for equation (33) and velocity (37). Left: c_1 (cross), c_2 (circle) and $4c_1 + c_2^2$ (dot). Middle: c_3 (cross) and c_4 (dot). Right: $\mathbb{E}(v)$ (cross), $\mathbb{E}(v^2)$ (circle) and $\mathbb{E}(v^3)$ (dot).

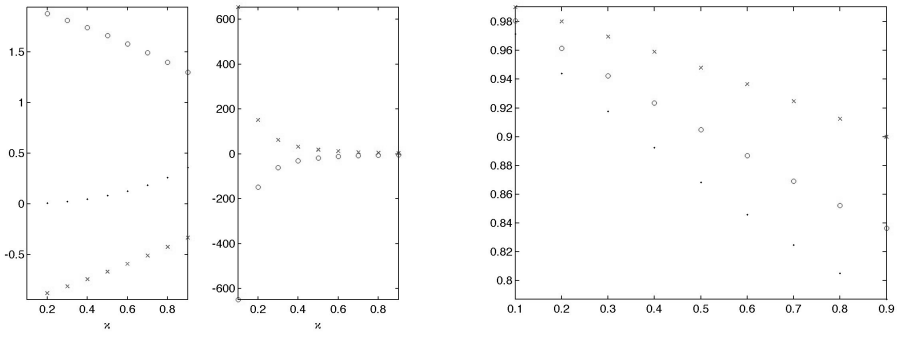

FIGURE 6. Transport coefficients $c_1, \ldots, c_4$ for equation (33) and velocity (38). Left: c_1 (cross), c_2 (circle) and $4c_1 + c_2^2$ (dot). Middle: c_3 (cross) and c_4 (dot). Right: $\mathbb{E}(v)$ (cross), $\mathbb{E}(v^2)$ (circle) and $\mathbb{E}(v^3)$ (dot).

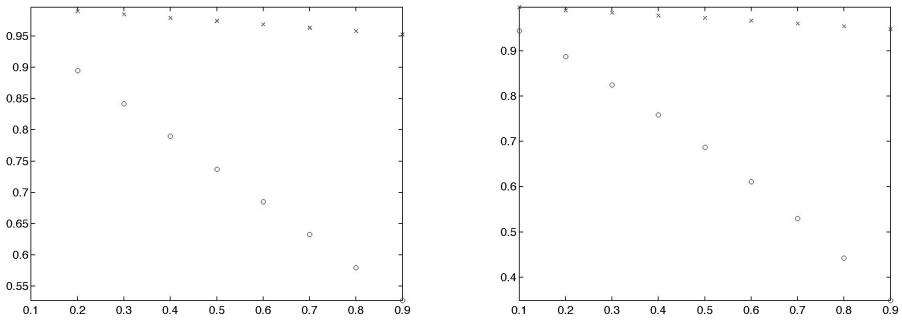

FIGURE 7. Eigenvalues λ_1 and λ_2 given by (35) for velocities (37) (left) and (38) (right), respectively.

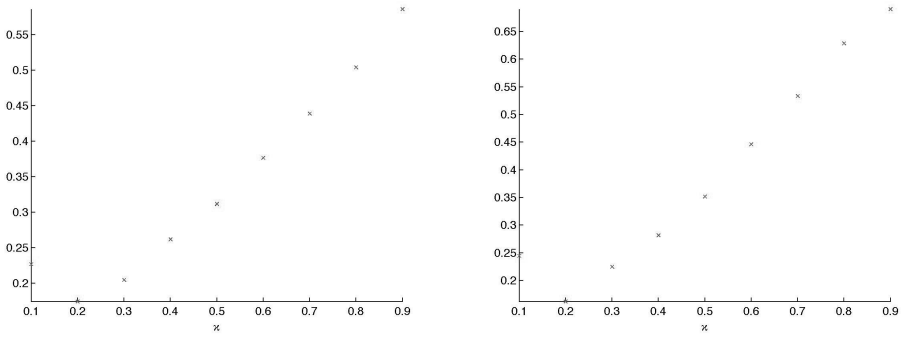

FIGURE 8. Degree of completion $x^* \in [0,1]$ at which a perturbation (0.1%) of the initial data leads to a density larger than one for velocities (37) (left) and (38) (right), respectively. The initial load of the assembly line is 85%.

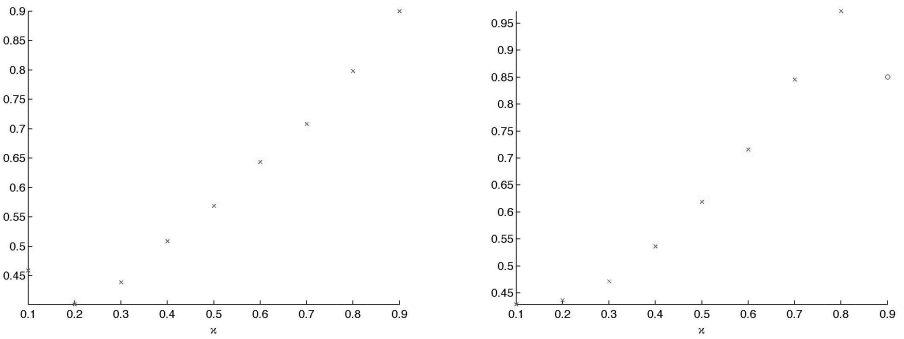

FIGURE 9. Degree of completion $x^* \in [0,1]$ at which a perturbation (0.1%) of the initial data leads to a density larger than one for velocities (37) (left) and (38) (right), respectively. Compared with Figure 8 the initial load of the assembly line is only 70%. The dot indicates that the density below is zero for $\kappa = 0.9$ in the right part of the figure.

5. Summary and future work

To model assembly lines, the automotive industry has to deal with large sets of data for part feeding processes. In this paper, we present an ansatz to model automotive assembly lines by using kinetic theory. To exhibit the same unidirectional flow of information as in the underlying particle model and reproduce the parabolic equations, we have derived a macroscopic model via hyperbolic conservation laws. Similar to [38] we discussed closure relations using Chapman-Enskog expansion without satisfactory results.

As consequence of the made assumptions on the microscopic interactions we have used moment approximations in Section 3.2, which are the starting point for studying the asymptotic behavior [37] of the model. To finally close the system we have used the Grad closure approach to derive an extended equilibrium function and to obtain the fluid dynamic equations (33), which are based on the statistical information of underlying data $\mathbf{\Phi}(a, n)$.

In Section 4 we have numerically discretized (33) and have simulated the density $\rho(t, x)$ for the evaluation and filtering out of a characteristic number for the long time behavior of the overall workload at automotive assembly lines.

We have outlined the capacity utilization ρ of the assembly line with degree of completion x. When prescribing the initial station averaged car distribution ρ_0 we are able to estimate the underlying velocity model $v(a)$. For example, for the typical load of an assembly line of $\rho_0 = 95\%$ we have found suitable values for κ in the interval $(0.3, 0.6)$. This information may be used to quantify the workload at the stations as well as rate of completion at stations. This is also a qualitative indicator of over- or underload at stations.

Summarizing, in this paper we present an approach using kinetic theory to assess workload in assembly lines. Especially the consideration of perturbations (e.g. dependency of not available parts, supply strategies) may be helpful when further extending the model. However, further data collection is required in order to give evidence to the predictions of the model.

Appendix A. Computations

We present some computations used in the derivation of the kinetic equations. Those computations can also be found in different context for example in [2, 34].

Consider N particles, $i = 1, \dots, N$ having each a state $X_i \subseteq \mathbb{R}$ and full state space $X = (X_i)_{i=1}^N \subseteq \mathbb{R}^N$. We only consider the following Monte-Carlo game for single particle interactions. For given $\Delta t > 0$ and with given frequency γ, we randomly pick a particle and a collision mechanism. Then, we change state from X to Y. Let $\beta_{c,i} = \frac{1}{N}\beta_c(X_i)$ for $c = 1, \dots, C$ and $i = 1, \dots, N$ be the (possibly state–dependent) probability to pick particle i and collision mechanism c. We require $\sum_{c=1}^{C} \beta_c(W) = 1$ for all $W \in \mathbb{R}^N$.

Denote by $Y = \xi_{c,i}(X)$ the new state of the system after collision at time $t + \Delta t$:

$$X(t+\Delta t) = \begin{pmatrix} X(t) & \text{with probability} & 1 - \gamma\Delta t & \\ \xi_{c,i}(X(t)) & \text{with probability} & \gamma\Delta t\beta_{c,i}(X(t)) & c = 1, \dots, C,\ i = 1, \dots, N \end{pmatrix}$$

In the assembly line model the collision mechanism $\xi_{c,i}$ only changes the state of particle i and hence we assume from now

$$\xi_{c,i}(X) = (X_1, \dots, \xi_c(X_i), \dots, X_N)$$

where $\xi_c : \mathbb{R}^N \to \mathbb{R}^N$ is the change of state for collision mechanism c. If we additionally assume, that the function $y \to \xi_c(y)$ is invertible, then, $\xi_{c,i}^{-1}(X) = (X_1, \dots, \xi_c^{-1}(X_i), \dots, X_N)$.

The microscopic dynamics will be rewritten in terms of the probability P. Let $P(X(t) = Z)$ be the probability that the state X of the system at time t equals Z

$$P(X(t+\Delta t) = Z) = (1-\gamma\Delta t)P(X(t) = Z) + \gamma\Delta t \sum_{c=1}^{C}\sum_{i=1}^{N} \beta_{c,i}(X(t))P(\xi_{c,i}(X(t)) = Z) \tag{39}$$

In order to rewrite (39), we assume there is a joint probability density function $F(t,x)$ such that $P(X(t) = Z) = F(t,Z)$ and $\int_{\mathbb{R}^{\ell\times N}} F(t,Z)dZ = 1$ where $dZ = dZ_1 \dots dZ_n$.

Using the molecular chaos assumption $F(X,t) = \prod_{i=1}^{N} f(t,X_i)$ with $\int f(t,X_i)dX_i = 1$ a formal computation leads to an equation for the single particle distribution. If each collision mechanism $\xi_c(\cdot)$ is invertible and if the molecular chaos assumptions holds true, then the single particle probability distribution function $f(t,x)$ with $x \in \mathbb{R}$ fulfills

$$f(t+\Delta t, x) = f(t,x) + \frac{\gamma\Delta t}{N}\left(\sum_{c=1}^{C} \beta_c(\xi_c^{-1}(x))|\det D\xi_c^{-1}(x)|f(t,\xi_c^{-1}(x)) - f(t,x)\right) \tag{40}$$

Due to equation (39) and upon integration on $Z_2, \dots, Z_N$, we have

$$\begin{aligned} F(t+\Delta t, Z) &= (1-\gamma\Delta t)F(t,Z) + \gamma\Delta t \sum_{c=1}^{C}\sum_{i=1}^{N} \int \beta_{c,i}(Y)F(t,Y)\delta(\xi_{c,i}(Y) - Z)dY \\ &= (1-\gamma\Delta t)F(t,Z) + \frac{\gamma\Delta t}{N}\sum_{c=1}^{C}\sum_{i=1}^{N} \beta_c(\xi_c^{-1}(Z_i)) \\ &\quad \cdot\ F(t, Z_1, \dots, \xi_c^{-1}(Z_i), \dots, Z_n)|\det D\xi_c^{-1}(Z_i)| \end{aligned} \tag{41}$$

$$\begin{aligned} f(t+\Delta t, Z_1) &= (1-\gamma\Delta t)f(t,Z_1) + \frac{\gamma\Delta t}{N}\int \sum_{c=1}^{C}\sum_{i=1}^{N} \beta_c(\xi_c^{-1}(Z_i))|\det D\xi_c^{-1}(Z_i)| \\ &\quad \times \quad f(t,\xi_c^{-1}(Z_i)) \prod_{j=1, j\neq i}^{N} f(t,Z_j)dZ_2 \dots dZ_N \\ &= (1-\gamma\Delta t)f(t,Z_1) + \frac{\gamma\Delta t}{N}\sum_{c=1}^{C} \beta_c(\xi_c^{-1}(Z_1))f(t,\xi_c^{-1}(Z_1))|\det D\xi_c^{-1}(Z_1)| \\ &\quad + \quad \frac{N-1}{N}\gamma\Delta t f(t,Z_1) \end{aligned} \tag{42}$$

Formal Taylor expansion in equation (40) yields a differential version leading to the kinetic equation.

If the function $X_i \to \xi_c(X_i)$ for all $c \in \{1, \dots, C\}$ is not invertible, then a similar kinetic equation can be derived. This case appears within the particle interaction at each station. Similarly, to the previous equation, we obtain

$$F(t+\Delta t, Z) = (1-\gamma\Delta t)F(t,Z) + \frac{\gamma\Delta t}{N}\sum_{c=1}^{C}\sum_{i=1}^{N}\int \beta_c(Y_i)\delta(\xi_c(Y_i)-Z_i)F(t,Z_1,\dots,Y_i,\dots,Z_n)dY_i \tag{43}$$

$$f(t+\Delta t, Z_1) = (1-\gamma\Delta t)f(t,Z_1) + \frac{\gamma\Delta t}{N}\int\sum_{c=1}^{C}\beta_c(Y_1)\delta(\xi_c(Y_1)-Z_1)f(t,Y_1)dY_1 + \frac{\gamma\Delta t}{N}\sum_{c=1}^{C}\sum_{i=1}^{N}\int f(t,Z_1)\beta_c(Y_i)\delta(\xi_c(Y_i)-Z_i)f(t,Y_i)dZ_i dY_i \tag{44}$$

$$f(t+\Delta t, Z_1) = (1-\gamma\Delta t)f(t,Z_1) + \frac{\gamma\Delta t}{N}\int\sum_{c=1}^{C}\beta_c(Y_1)\delta(\xi_c(Y_1)-Z_1)f(t,Y_1)dY_1 + \frac{N-1}{N}\gamma\Delta t f(t,Z_1) \tag{45}$$

Finally, we obtain for non–invertible changes of state ξ_c and $x \in \mathbb{R}$

$$f(t+\Delta t, x) = f(t,x) + \frac{\Delta t\gamma}{N}\left(\sum_{c=1}^{C}\int_{\mathbb{R}^\ell}\beta_c(y)\delta(X-\xi_c(Y))f(t,Y)dY - f(t,x)\right). \tag{46}$$

Clearly, a combination of both processes is possible where part of the change of state is reversible (invertible) and part not. The corresponding kinetic equation is then a combination of the terms of equation (40) and (46). This is the case for the presented production process where $C = 3$ and $c \in \{1, 2\}$ are invertible processes but $c = 3$ is not.

Acknowledgements. This work has been supported by DFG Cluster of Excellence EXC128, the BMBF KinOpt Project, DAAD 54365630 and DAAD 55866082.

References

[1] G. Albi and L. Pareschi, *Binary interaction for the simulation of flocking and swarming dynamics*, Multiscale Modeling and Simulation, 11 (2013), pp. 1–29.

[2] D. Armbruster, P. Degond, and C. Ringhofer, *A model for the dynamics of large queuing networks and supply chains*, SIAM Journal on Applied Mathematics, 66 (2006), pp. 896–920.

[3] D. Armbruster, D. Marthaler, and C. Ringhofer, *Kinetic and fluid model hierarchies for supply chains*, Multiscale Modeling and Simulation, 2(1) (2003), pp. 43–61.

[4] D. Armbruster, D. Marthaler, C. Ringhofer, K. Kempf, and T.-C. Jo, *A continuum model for a re-entrant factory*, Operations Research, 54(4) (2006), pp. 933–950.

[5] D. Armbruster and C. Ringhofer, *Thermalized kinetic and fluid models for re-entrant supply chains*, SIAM Journal on Multiscale Modeling and Simulation, 3 (2005).

[6] D. Armbruster and R. Uzsoy, *Continuous dynamic models, clearing functions, and discrete-event simulation in aggregate production planning*, (2012).

[7] J. Banks, J. Carson II, and B. Nelson, *Discrete event system simulation*, (1999).

[8] A.-L. Barabasi and R. Albert, *Emergence of scaling in random networks*, Science, 286 (1999), pp. 509–512.
[9] S. Battiston, D. Delli-Gatti, M. Gallegati, B. Greenwald, and J. E. Stiglitz, *Credit chains and bankruptcy propagation in production networks*, Journal of Economic Dynamics and Control, 31 (2007), pp. 2061–2084.
[10] N. Bellomo, A. Bellouquid, and D. Knopoff, *From the Microscale to Collective Crowd Dynamics*, SIAM Multiscale Modeling and Simulation, 11 (2013), pp. 943–963.
[11] N. Bellomo and F. Brezzi, *Traffic, crowds, and swarms*, Mathematical Models and Methods in Applied Sciences, 18 (2008), pp. 1145–1148.
[12] ——, *Mathematics and complexity of multi-particle systems*, Mathematical Models and Methods in Applied Sciences, 22 (2012).
[13] N. Bellomo and C. Dogbe, *On the modelling of traffic and crowds a survey of models, speculations, and perspectives*, Society for Industrial and Applied Mathematics Review, 53 (2011), pp. 409–463.
[14] N. Bellomo, D. Knopoff, and J. Soler, *On the difficult interplay between life, "complexity", and mathematical sciences*, Mathematical Models and Methods in Applied Sciences, 23 (2013), pp. 1861–1913i.
[15] N. Bellomo and J. Soler, *On the mathematical theory of the dynamics of swarms viewed as complex systems*, Mathematical Models and Methods in Applied Sciences, 22 (2012), pp. 1861–1913i.
[16] D. Brockmann, *Anomalous diffusion and the structure of human transportation networks*, The European Physical Journal Special Topics, 157(1) (2008).
[17] C. Cercignani, *The Boltzmann equation and its applications*, (1988).
[18] C. Cercignani, R. Illner, and M. Pulvirenti, *The mathematical theory of dilute gases*, (1994).
[19] R. M. Colombo and A. Corli, *On a class of hyperbolic balance laws*, Journal of Hyperbolic Differential Equations, 1 (2004).
[20] S. Cordier, L. Pareschi, and G. Toscani, *On a kinetic model for a simple market economy*, Journal of Statistical Physics, 120 (2005), pp. 253–277.
[21] C. M. Dafermos, *Hyperbolic conservation laws in continuum physics*, 325 (2005), pp. xx+626.
[22] C. D'Apice, S. Göttlich, M. Herty, and B. Piccoli, *Modeling, simulation, and optimization of supply chains*, (2010), pp. x+206. A continuous approach.
[23] P. Degond, S. Goettlich, A. Klar, M. Seaid, and A. Unterreiter, *Derivation of a kinetic model from a stochastic particle system*, Kinetic and related models, 1 (2008), pp. 557–572.
[24] P. Degond, S. Göttlich, M. Herty, and A. Klar, *A network model for supply chains with multiple policies*, SIAM Multiscale Modeling and Simulation, 6 (2007), pp. 820–837.
[25] P. Degond and S. Motsch, *Continuum limit of self-driven particles with orientation interaction*, Mathematical Models and Methods in Applied Sciences, 18 (2008), pp. 1193–1215.
[26] F. Della Rossa, C. D'Angelo, and A. Quarteroni, *A distributed model of traffic flows on extended regions*, Networks and Heterogeneous Media, 5 (2010), pp. 525–544.
[27] B. Dubroca and J. L. Feugeas, *Entropic moment closure hierarchy for the radiative transfer equation*, Journal of Quantitative Spectroscopy and Radiative Transfer, 329 (1999), pp. 915–920.
[28] J. Golz, R. Gujjula, H. Günther, S. Rinderer, and M. Ziegler, *Part feeding at high-variant mixed-model assembly lines*, Flexible Services and Manufacturing Journal, 24 (2012), pp. 119–141.
[29] S. Göttlich, M. Herty, and A. Klar, *Network models for supply chains*, Communications in Mathematical Sciences, 3 (2005), pp. 545–559.
[30] S. Göttlich, M. Herty, and A. Klar, *Modelling and optimization of supply chains on complex networks*, Communications in Mathematical Sciences, 4 (2006), pp. 315–330.
[31] S. Göttlich, M. Herty, and C. Ringhofer, *Optimization of order policies in supply networks*, European Journal of Operational Research, 202 (2010), pp. 456–465.
[32] B. D. Greenshields, *A study of traffic capacity*, Highway Research Board, 14 (1935), pp. 448–477.
[33] M. Herty, R. Illner, A. Klar, and V. Panferov, *Qualitative properties of solutions to systems of Fokker-Planck equations for multilane traffic flow*, Transport Theory and Statistical Physics, 35 (2006), pp. 31–54.

[34] M. Herty and C. Ringhofer, *Averaged kinetic models for flows on unstructured networks*, AIMS Kinetic and Related Models, 4 (2011), pp. 1081–1096.
[35] A. Klar and R. Wegener, *Kinetic derivation of macroscopic anticipation models for vehicular traffic*, SIAM Journal on Applied Mathematics, 60 (2000), pp. 1749–1766 (electronic).
[36] C. D. Levermore, *Relating Eddington factors to flux limiters*, Journal of Quantitative Spectroscopy and Radiative Transfer, 31 (1984), pp. 149–160.
[37] G. Toscani, *Kinetic models of opinion formation*, Communications in Mathematical Sciences, (2006), pp. Vol 4 481–496.
[38] A. Unver, C. Ringhofer, and D. Armbruster, *A hyperbolic relaxation model for product flow in complex production networks*, AIMS Journal of Discrete and Continuous Dynamical Systems, (2009), pp. 791–800.